THE LOOPED ADHESIVE STRIP:
An Example of Coplanar Delamination Interaction

W. J. Bottega
Dept. of Mechanics and Materials Science
Rutgers University
Piscataway, N.J.

Introduction

The phenomenon of peeling and debonding of thin layers is a subject of interest to those concerned with adhesives, thin films, and layered materials. In recent years much attention has been focused on such problems as a result of increased interest and application of advanced composites and thin film coatings. (See for example ref. 1. An extensive list of references pertaining to the subject can be found therein.) A related problem which is of interest for its own sake but also represents a simple example of a tangled adhesive strip and of coplanar delamination interaction, is the problem of a looped adhesive strip. This is the subject of the present study.

We consider here the problem of an elastic strip which possesses an adherend on (at least) one of its surfaces. If the strip is deformed so that two portions of such a surface are brought into contact, a portion of the strip becomes bonded and a loop is formed (Figure 1). We shall be interested in determining the equilibrium configuration of such a strip and investigating the behavior of the strip when its edges are pulled apart.

The problem shall be approached as a moving interior boundary problem in the calculus of variations with the strip modeled as an inextensible elastica and the bond strength characterized by its surface energy.* A Griffith type energy criterion shall be employed for debonding, and solutions corresponding to the problem of interest obtained. The solution obtained will be seen to predict the interesting phenomenon of "bond point propagation", as well as the more standard peeling type behavior. Numerical results demonstrating the phenomena of interest are presented as well and will be seen to reveal both stable and unstable propagation of the boundaries of the bonded portion of the strip, depending upon the loading conditions.
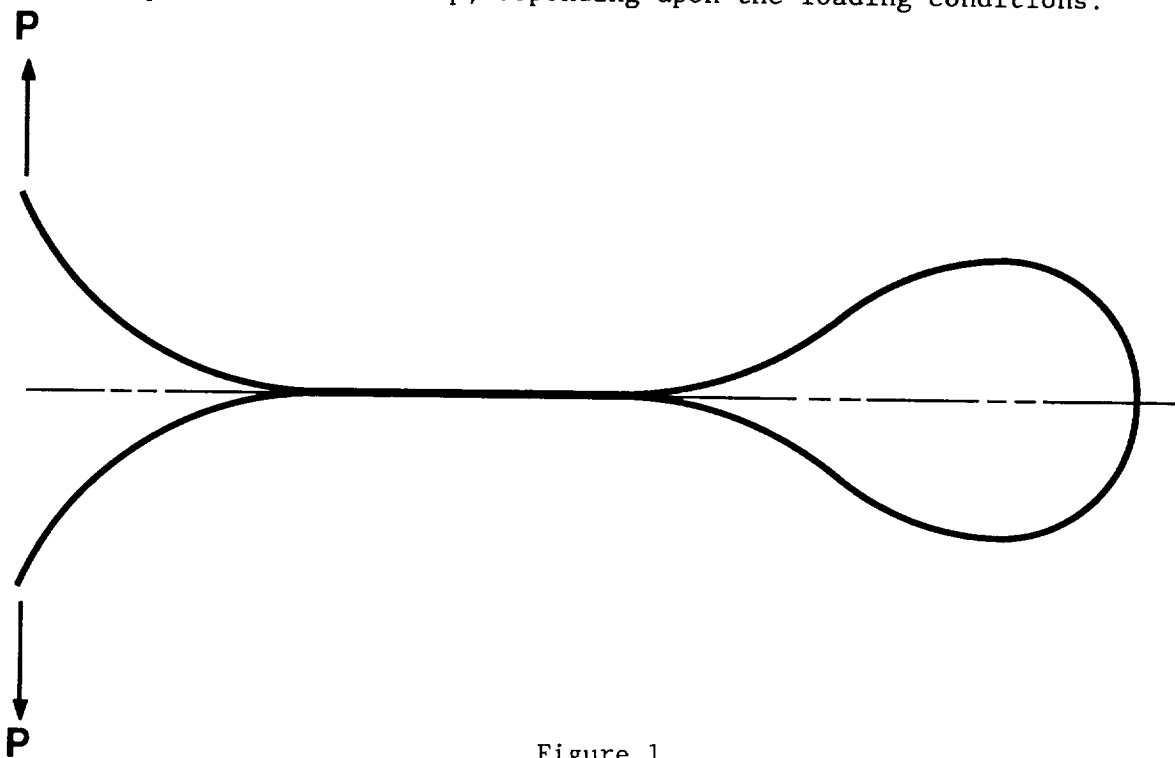

P

P

Figure 1

*Bottega, W.J.: Peeling and Bond Point Propagation in a Self-Adhered Elastica. To appear in Quart. J. Mech. and Appl. Math.

68

Formulation of the Problem

Consider a thin elastic strip which possesses an adherend on one of its surfaces, and let the strip be closed on itself in a symmetric manner such that there exists a region in the plane of symmetry where the strip is bonded to itself (Figure 1). Additionally, let the edges of the strip be subjected to equal and opposite forces as shown. As a result of the inherent symmetry of the problem, only half of the strip need be considered in the ensuing analysis (Figure 2). The strip thus consists of a lifted segment, a bonded segment, and a looped segment. In what follows, all length scales have been normalized with respect to the half length, L, of the entire strip.

We shall identify each point on the centerline of the strip by its normalized arc length, s, measured from the edge at which the external force is applied. In so doing, the half strip will be divided into four regions; corresponding to the lifted segment defined on $0 \leq s \leq a$, $a \leq s \leq b$ corresponding to the bonded segment , with the looped segment of the strip divided into two regions, defined by $b \leq s \leq s^*$ preceding the associated inflection point, s^*, and $s^* \leq s \leq 1$ following the inflection point. We shall be interested in assessing the behavior of the above system as a function of the magnitude of the applied load or the corresponding edge displacement.

Let us first define the right handed cartesian coordinate system (x,y) as shown in the figure. In addition, let us define the angle $\theta(s)$ which measures the angle that the tangent of the strip at point "s" makes with the x-axis as s increases (see Figure 2). One then may easily find the relations

$$x(s_2)-x(s_1) = \int_{s_1}^{s_2} \cos \theta \, ds \quad \text{and} \quad y(s_2) -y(s_1) = \int_{s_1}^{s_2} \sin \theta \, ds . \qquad \text{(i-a,b)}$$
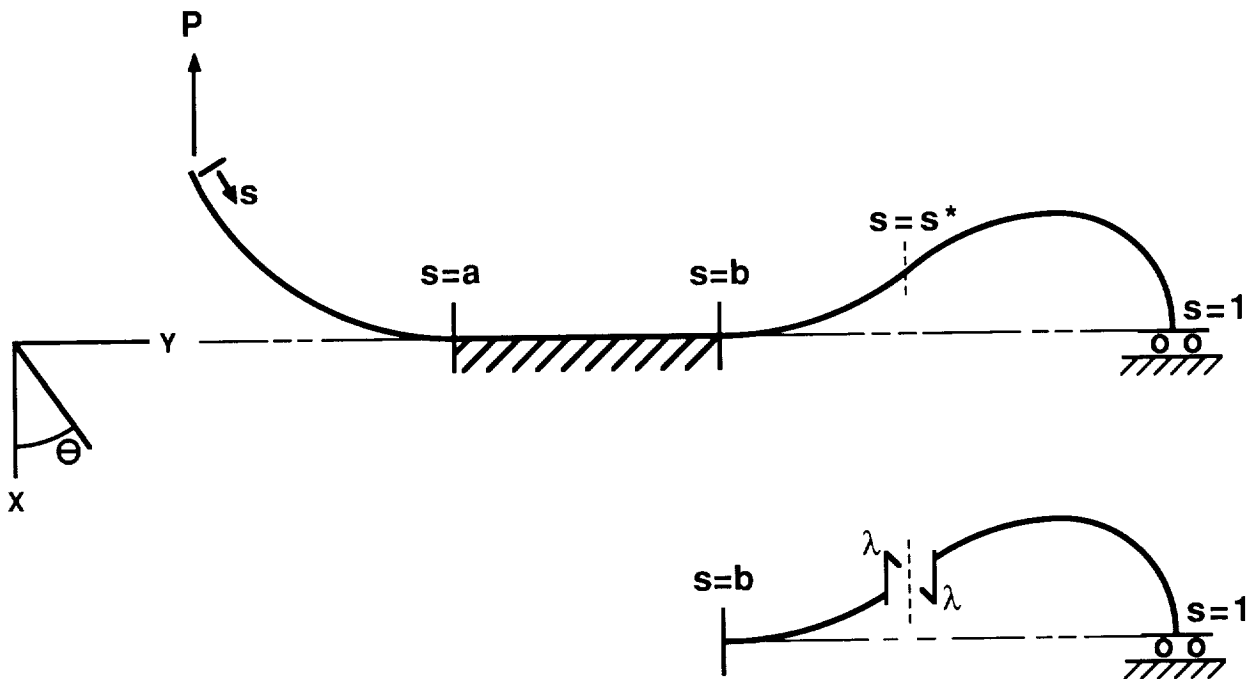

Figure 2

Energy Functional

As we shall approach the problem as a moving interior boundary value problem in the calculus of variations, we next define the energy functional $\prod$ given in Table 1 where $U^{(i)}$ corresponds to the normalized strain energy of the segment of the strip defined on the domain D_i, and is seen to be comprised solely of bending energy as the elastica is assumed to be inextensible. The strain energy of the (perfectly) bonded segment of the strip, i.e., the portion of the strip on $[a,b]$, is thus seen to vanish identically. The functional W corresponds to the normalized work done by the applied load. In that expression, $P = \bar{P}L^2/\bar{D}$ corresponds to the normalized counterpart of the magnitude of the applied load, $\bar{P}$, and $\bar{D}$ represents the bending stiffness of the strip. The functional Γ corresponds to the "delamination energy" where $\gamma - \bar{\gamma}L^2/\bar{D}$ represents the normalized counterpart of the surface energy of the bond, $\bar{\gamma}$, while a_0 and b_0 correspond to the initial values of a and b respectively.

Finally, we introduce the constraint functional Λ, with Lagrange multiplier λ, which constrains the deflections of the segments of the strip on D_3 and D_4 to be continuous at $s - s*$. The functions $x_3(s*)$ and $x_4(s*)$ may be expressed in terms of θ by eq. (i-a). Thus,

$$\Lambda - \lambda \int_b^{s*} \cos \theta \, ds + \lambda \int_{s*}^1 \cos \theta \, ds \quad . \tag{2e'}$$

We note that the inclusion of Λ is equivalent to treating the segments on D_3 and D_4 as separate structures and including the work done by the internal force λ, at $s - s*$. It may be seen that the line of action of this force must be parallel to the x-axis as a result of the support condition at $s - 1$ (see Figure 2).

Table 1

$$\prod = \sum_{i=1}^{4} U^{(i)} - W + \Gamma - \Lambda \tag{1}$$

where:

$$U^{(i)} = \int_{D_i} \frac{1}{2}(d\theta/ds)^2 \, ds \tag{2a}$$

$$U^{(2)} \equiv 0 \tag{2b}$$

$$W = -P \, x \, (o) = P \int_o^a \cos \theta \, ds \tag{2c}$$

$$\Gamma = 2\gamma(a-a_0) - 2\gamma(b-b_0) \tag{2d}$$

$$\Lambda = \lambda[x_3(s*) - x_4(s*)] \tag{2e}$$

70

The Governing Equations

The governing differential equations, boundary conditions, matching conditions and transversality conditions for the problem of interest are found by invoking the principle of stationary potential energy as shown in Table 2 below. In equation (3), the parameter δ represents the variational operator.

The transversality conditions (7a,b,c) result from the moving boundaries during peeling or bonding of the strip and thus are associated with equilibrium configurations of the system during these processes.

The intermediate boundaries a, b and s*, as well as the inflection point angles $\bar{\alpha}$ and $\alpha*$ are found as part of the solution to the problem.

Table 2

Principle of Stationary P.E.: $\delta\Pi = 0$ (3)

(1) into (3):

$$\frac{1}{2}(\frac{d\theta_i}{ds})^2 + P_i(\cos\alpha_i - \cos\theta_i) = 0, \quad (i = 1,3,4) \quad (4)$$

$$\theta_2 = \pi/2$$

where: $\theta_1 = \bar{\theta} \equiv \pi - \theta$, $\alpha_1 = \bar{\alpha} \equiv \bar{\theta}(0)$, $P_1 = P$,

$$(5)$$

$$\theta_{2,3,4} = \theta, \quad \alpha_{3,4} = \alpha* \equiv \theta(s*), \quad P_{3,4} = \lambda$$

with B.C.s and M.C.s:

$$\theta_1(a) = \theta_3(b) = \pi/2, \quad (6a,b)$$

$$\theta_4(1) = 0 \quad (6c)$$

$$\theta_3(s*) = \theta_4(s*) = \alpha* \quad (6d)$$

$$\int_b^{s*} \cos\theta \, ds = -\int_{s*}^1 \cos\theta \, ds \quad (6e)$$

and T.C.s:

$$G(a^-) \equiv \frac{1}{2}(\frac{d\theta_1}{ds})^2 \Big|_{s=a^-} = 2\gamma \quad (7a)$$

$$G(b^+) \equiv \frac{1}{2}(\frac{d\theta_3}{ds})^2 \Big|_{s=b^+} = 2\gamma \quad (7b)$$

$$\frac{d\theta_3}{ds}\Big|_{s=s*} = \frac{d\theta_4}{ds}\Big|_{s=s*} = 0 \quad (7c)$$

71

Criteria for Propagation of the "Bond Zone" Boundaries

The conditions (7a) and (7b) establish the bond zone boundaries during their propagation and state that the values of a and b corresponding to equilibrium configurations of the system during propagation of each interior boundary are those for which the bending energy densities at the point $s = a^-$ and $s = b^+$ are just balanced by the energy of the bond. In this context the quantities $G(a^-)$ and $G(b^+)$ may be identified as the "energy release rates" at the bond zone boundaries. The above suggests the criteria for propagation of the boundaries of the bonded region of the elastica, as listed in Tables 3a and 3b.

Peeling

If, for some initial $a = a_0$, eqn. (8a) is satisfied, no peeling will occur and a will remain at its initial value a_0 with the lifted segment bending away from the plane of symmetry. If, for some initial $a = a_0$, eqn. (8b) is satisfied, the lifted segment of the strip peels away from the plane of symmetry such that the value of a increases until the corresponding equality (7a) is satisfied.

Following the above reasoning, we conclude that for the loop to maintain its initial configuration, conditions must be such that eqn. (9a) is satisfied. If eqn. (9b) holds, the loop would open as a result of excess bending energy at its edge, with b taking on smaller values until the energy of deformation is just balanced by the energy of the bond.

Table 3a

Criteria for Propagation
of Bond Zone Boundaries:

Peeling:

If $G\{a^-_o\} < 2\gamma$	No Peeling	(8a)
If $G\{a^-_o\} > 2\gamma$	Peeling until a satisfies equality (7a)	(8b)

Similarly,

If $G\{b_o^+\} < 2\gamma$	Loop maintains initial configuration	(9a)
If $G\{b_o^+\} > 2\gamma$	Loop grows (b decreases until b satisfies equality (7b)	(9b)

Bond Point Propagation

If conditions are such that the bending energy $G\{a^-\}$ is sufficiently large while $G\{b_o^+\}$ is sufficiently small, the bond zone boundary "a" will increase while b remains at its initial value until $a = b^-$. At this stage, as the resultant bending moment m_{ba} acting at the bond point satisfies eqn (10) (Table-3b), and hence acts in a clockwise sense, tending to rotate the strip in this sense, while simultaneously there exists a sufficient surplus of bond energy to counter the bending energy of the loop and induce bonding at the loop edge, the strip behaves locally as if rolling over its counterpart and the "bond point" $s = a = b$ will propagate such that the loop closes and shrinks until the corresponding equality (7b) is satisfied. At this point the surplus bond energy is depleted and bonding at $s = b^+$ can no longer occur. Equivalently, the growth condition (9b) as well as (8b) will become satisfied and conditions will then be such that propagation can occur in both directions simultaneously. Under such conditions, the loop will expire and the strip will separate completely.

Table 3b

"BOND POINT PROPAGATION":

If (9a) and (8b) satisfied, $a \rightarrow b_o^-$.

Resultant Bending Moment:

$$m_{ba} = [[d\theta/ds]]_{s=b} = [d\theta/ds]_{s=b^+} - [d\theta/ds]_{s=b^-} < 0 \qquad (10)$$

(thus, m_{ba} is clockwise)

Thus, "bond point" propagates until equality (7b) satisfied and loop expires.

Basic Integrals

The nonlinear differential equations (4) governing the local rotations on each segment of the strip are seen to be of standard form, which upon solving for ds, integrating over the corresponding domain, and using the transformation given by (11), results in expressions for the segment arc lengths ℓ_i (i=1,3,4) in terms of the inflection point angles and corresponding external or internal loads as given in Table 4. We note that these lengths will vary as a result of bonding and debonding. The functionals $F(q,\Phi)$ and $F_k(q)$ in eqns. (12) correspond to elliptic integrals of the first kind and complete elliptic integrals of the first kind, respectively, defined by

$$F(q_i,\Phi) = \int_0^\Phi \frac{d\phi_i}{\sqrt{1-q_i^2\sin^2\phi_i}} \quad \text{and} \quad F_k(q_i) = F(q_i,\pi/2) \quad . \qquad \text{(ii-a,b)}$$

We shall first consider equilibrium configurations of the lifted segment ($\theta \in D_1$) and of the looped segment ($\theta \in D_3 + D_4$) separately, and then examine their interaction.

Table 4

BASIC INTEGRALS

Transformation:

$$\sin(\theta_i/2) = q_i \sin \phi_i \qquad \text{(11a)}$$

$$q_i = \sin(\alpha_i/2) \quad (i = 1,3,4) \qquad \text{(11b)}$$

(11) into (4), solving for ds and integrating ⇒

segment arc lengths ℓ_i :

$$\ell_1 = a = [F_k(q_1) - F(q_1,\hat{\Phi}_1)]/\sqrt{P} \qquad \text{(12a)}$$

$$\ell_3 = s^* - b = [F_k(q^*) - F(q^*,\hat{\Phi}_3)]/\sqrt{\lambda} \qquad \text{(12b)}$$

$$\ell_4 = 1-s^* = F_k(q^*)/\sqrt{\lambda} \qquad \text{(12c)}$$

$$\text{where} \quad q_3 = q_4 = q^* \qquad \text{(13a)}$$

$$\hat{\Phi}_i = \sin^{-1}\{1/(q_i\sqrt{2})\} \qquad \text{(13b)}$$

$F(q,\Phi)$ – Elliptic Integral of 1st Kind

$F_k(q_i)$ – Complete E.I. of 1st Kind

Behavior of the Lifted Region

The deflection of the edge of the strip at which the load is applied is found by solving equation (4a) for $d\theta_1/ds$ and substituting the resulting expression into equation (i-a), with appropriate limits of integration. Then, upon incorporating the transformation (13), we obtain the load edge deflection, Δ_o, as given in Table 5, where

$$E(q_i,\Phi) = \int_o^\Phi \sqrt{1-q_i^2 \sin^2 \phi_i} \ d\phi_i \qquad \text{and} \qquad E_k(q_i) \equiv E(q_i,\pi/2) \quad , \quad \text{(iii-a,b)}$$

correspond to elliptic integrals of the second kind, and complete elliptic integrals of the second kind, respectively. The explicit form of the transversality condition at the "trailing edge" of the bonded region (i.e., at s = a) may be found by solving equation (4a) for $[d\theta_1/ds]_{s=a}$ and substituting the resulting expression into (7a). We then have the condition which (implicitly) defines the location of the trailing edge of the "bond zone", during peeling, given by eqn. (15).

Substitution of equation (15) into equation (12), with i = 1, and equation (14) gives explicit relations for the magnitude of the applied load as a function of "a" and the normalized load point deflection as a function of "a" respectively, with the load point rotation $\bar{\alpha}$ a parameter. Specific results corresponding to selected values of γ will be presented in a later section.

Table 5

BEHAVIOR OF LIFTED REGION

LOAD POINT DEFLECTION:

$$\Delta_o \equiv -x\big|_{s=o} = \frac{1}{\sqrt{P}}\{[2E(q_1,\hat{\ast}_1) - F(q_1,\hat{\ast}_1)]$$

$$- [2E_k(q_1) - F_k(q_1)]\} \qquad (14)$$

where $E(q,\ast)$ – Elliptical Integral of 2nd Kind

$E_k(q_i)$ – Complete E.I. of 2nd Kind

T.C. @ s = a^- (7a) becomes

$$P = -2\gamma/\cos \bar{\alpha} \qquad (\pi/2 < \bar{\alpha} \leq \pi) \qquad (15)$$

75

Equilibrium Configurations of the Loop

The angle which measures the rotation of the tangent of the loop at its inflection point $s = s*$ is found by imposing the condition (6e). Thus, solving equations (4b) and (4c) for $d\theta/ds$, substituting the resulting expressions into the left and right hand sides of (6e) respectively, noting (6d) and incorporating the transformation (11) for $i = 3,4$ we obtain the condition given by (16) below where as defined earlier, $\alpha* = \alpha_3 = \alpha_4$ and $q* = q_3 = q_4$. It may be seen from equation (16) that $\alpha*$ is independent of the size of the loop, of the material and geometric properties of the strip and bond, and of the magnitude of the applied load, and thus is a "characteristic angle" of the problem. Equation (16) may be solved numerically to yield the value of $\alpha*$ as given below.

The total (half) arc length of the loop, ℓ, is simply comprised of the sum of the lengths of its constituent segments. Thus, adding equations (12b) and (12c) yields the relation for ℓ, given by (18). The relative portions of the loop corresponding to its constituent segments are then found by dividing eqns. (12b) and (12c) by (18). We thus have

and
$$\ell_3/\ell = [F_k(q*) - F(q*,\Phi*)]/[2F_k(q*) - F(q*,\Phi*)] \qquad (19a')$$

$$\ell_4/\ell = F_k(q*)/[2F_k(q*) - F(q*,\Phi*)] , \qquad (19b')$$

which are seen to correspond to "characteristic length ratios" of the problem. The above ratios may be evaluated, using the computed value of $\alpha*$, to yield the values given at the bottom of Table 6.

Table 6

EQUILIBRIUM CONFIGURATIONS OF THE LOOP

Imposing (6e):

$$2[2E_k(q*) - F_k(q*)] = 2E(q*, \bullet*) - F(q*, \bullet*) \qquad (16)$$

(where $\bullet* = \hat{\bullet}_3 = \hat{\bullet}_4$).

Solving (16) yields "characteristic angle" of inflection point

$$\alpha* = 117.54\cdot \quad \text{(for any loop size and}$$
$$\text{mat'l./geom. props.)} \qquad (17)$$

(12b) + (12c) → loop (half) arc length ℓ:

$$\ell = \ell_3 + \ell_4 = [2F_k(q*) - F(q*, \bullet*)]/\sqrt{\lambda} \qquad (18)$$

(12b,c)/(18) → "Characteristic Arc Length Ratios":

$$\ell_3/\ell = 0.3254 \text{ and } \ell_4/\ell = 0.6746 \qquad (19a,b)$$

(for any loop size and mat'l./geom. props.)

76

Debonding of the Looped Segment

We may next consider equilibrium configurations of the looped segment of the strip as it opens (debonds) by evaluating the explicit form of the transversality condition at $s = b^+$ in a manner analogous to that done earlier for the lifted segment. Doing so we find that during opening of the loop, the condition (7b) takes the form given by eq'n.(20) where $\alpha*$ is given by (17). Since, as discussed earlier, $\alpha*$ is a "characteristic angle" (i.e., it maintains a fixed value for any equilibrium configuration of the loop,) it is seen from the above expression that the internal force λ maintains a constant value during debonding of the loop.

Substitution of (20) into equation (18) yields a critical value of the loop length given by equation (21) below, with the inequalities (9a,b) now interpreted in terms of the arc length of the loop; e.g. - (22a,b).

It may be noted that a minimum value of the normalized bond energy is required for the elastica to remain adhered to itself. This value $\gamma - \gamma_{min}$ corresponds to the limiting case where the loop traverses the entire strip and is in self-contact only at the loading edge $s = 0$ (i.e., it corresponds to the limiting case when $\ell_{cr} - 1$). Upon employing the result (19) we find the desired value given below. Adherends whose normalized bond energies possess magnitudes which are below this value are thus not "strong enough" to maintain a self-adhered configuration.

<div align="center">

Table 7

T.C. @ $s = b^+$ (7b) becomes:

</div>

$$\lambda = -2\gamma/\cos \alpha* \quad (= \text{constant for given } \gamma) \qquad (20)$$

(20) into (18):

$$\ell = [2F_K(q*) - F(q*, *)]\sqrt{(-\cos\alpha*)/2\gamma} \qquad (21)$$

If $\ell > \ell_{cr}$ No debonding of loop occurs   (22a)

If $\ell < \ell_{cr}$ Debonding of loop occurs

      ℓ increases (b decreases) until $\ell = \ell_{cr}$ (22b)

$$\ell_{cr} = 1 \Rightarrow \gamma = \gamma_{min} = 2.292 \qquad (23)$$

Effective Bond Strength and Propagation Behavior

A plot of ℓ_{cr} versus γ is displayed in Figure 3. It may be observed from the figure that the amount of "effective bond strength" gained, as measured by the relative decrease in ℓ_{cr}, significantly decreases as γ is increased beyond 200.

Peeling and Bond Point Propagation

The above solution offers the following scenario for a looped adhesive strip with given $\gamma > \gamma_{min}$ existing in an initial configuration such that $\ell_o = 1-b_o > \ell_{cr}$ (or equivalently $b_o < b_{cr} = 1-\ell_{cr}$), with an initial lift zone size of $\ell_1 = a_o$. As P is increased the corresponding value of $\alpha_1 = \alpha$ is increased according to equation (12a), with the associated deflection Δ_o varied according to equation (14). This process is continued until equation (15) is satisfied at which point peeling begins with the "trailing edge" of the "bond zone" s = a propagating (and ℓ_1 increasing). As the initial loop length ℓ_o is larger than the critical length, the loop edge boundary of the bond zone remains at its initial value until a = b_o. At this point if conditions are such (equation (15) satisfied) that peeling continues, the bond point a = b propagates with ℓ decreasing (b increasing). During this phase the values of $\alpha*$, ℓ_3/ℓ, and ℓ_4/ℓ maintain the values given by (17) and (19a,b) respectively. The loop thus shrinks in size during this phase, with its geometry evolving through successive self-similar shapes (as if the strip were being pulled through a rigid clamp at s = b). This process continues until $\ell = \ell_{cr}$, at which point conditions are such that peeling may occur at both s = b^- and s = b^+ (i.e., in both directions) simultaneously. At this instant the loop is terminated and the surfaces on each side of the plane of symmetry separate. Results corresponding to specific values of γ are presented next.
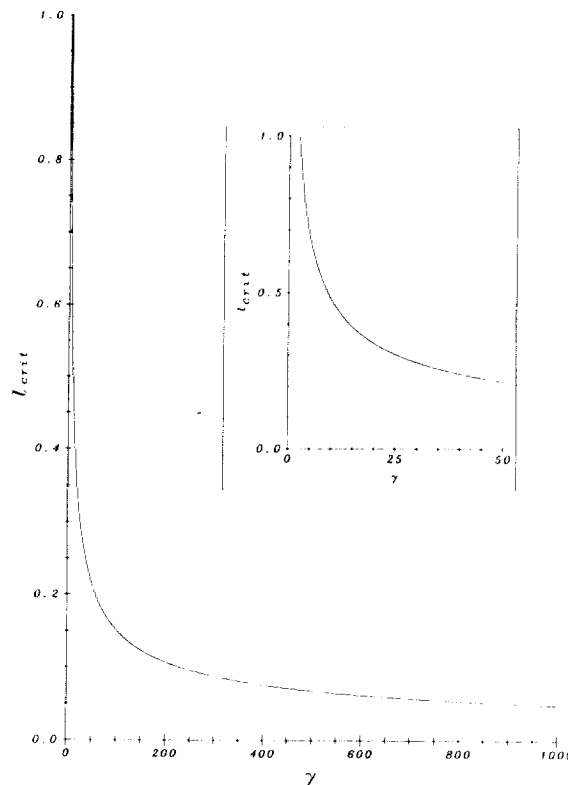

Fig. 3. Variation of Critical Loop (Half) Length with Normalized Bond Energy

Numerical Results

Results are presented corresponding to selected values of the normalized bond energy. Specifically, we consider the strip/adherend systems whose material and geometric properties are characterized by the values γ = 5, 10, 50, 100, and 1000 respectively.

The projections of the associated lift zone/bond point "propagation paths" in the Δ_o-a, P-a and P-Δ_o spaces are calculated and are displayed in Figures 4-7. Each curve is terminated at the critical values a = b_{cr} = 1-ℓ_{cr}, which are given by the values b_{cr} = .3230, .5213, .7859, .8486, and .9522 for the respective values of γ considered. The prepropagation load-deflection behavior of lift zone segments corresponding to initial lengths of a_o = 0.25 and a_o - 0.50 are also displayed in Figure 6. Finally, the variation of the magnitude of the internal force λ, as a function of the loop length ℓ, is displayed in Figure 8.

It may be seen from the figures that propagation of the lift zone boundary or bond point occurs in a stable manner for a deflection controlled test, and in an unstable and "catastrophic" manner for a force controlled test. The following example illustrates the general behavior of the self-adhered elastica.
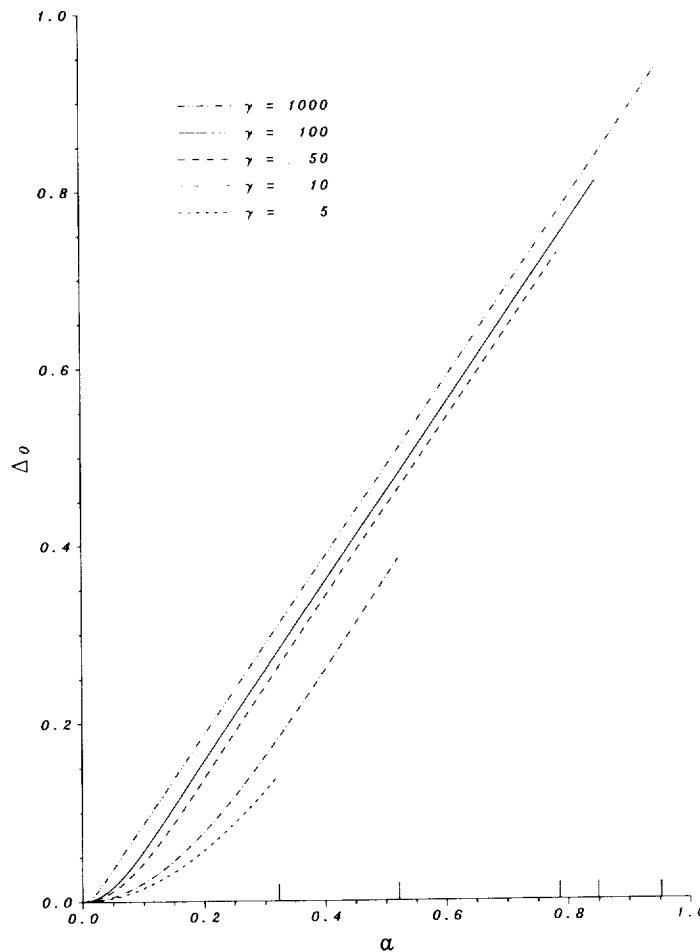

Fig. 4. Lift Zone/Bond Point Propagation Paths (γ - 5, 10, 50, 100, 1000):
Load Edge Deflection vs. Bond Zone Boundary

Let us consider a strip/adherend combination with $\gamma = 50$ which is initially configured such that $a_o = 0.25$ and $b_o = 0.60$. It may be observed that a system characterized by one of the smaller values of γ considered could not maintain a loop size this small (b_o this large) and that for such a system the loop edge boundary, b, would immediately decrease to its corresponding critical value. Returning to the previously defined case ($\gamma = 50$), the system initially follows the prepropagation path for $a_o = 0.25$ in Figure 6, as P and Δ_o increase from the origin. During this phase, the system simultaneously follows a purely vertical path, corresponding to $a = 0.25$, in the Δ_o-a and P-a spaces (Figures 4 and 5). The system continues to behave in this fashion until the propagation path corresponding to $\gamma = 50$ is intercepted. At this point the lifted segment of the strip has accumulated enough bending energy at the bond zone boundary $s = a^-$, for the lift zone to propagate. We note that as $\ell_o > \ell_{cr}$ ($b_o < b_{cr}$) the bending energy of the looped segment at $s = b^+$ is insufficient for propagation so b remains at its initial value. Let us first consider the case where the load edge deflection, Δ_o, is controlled. For this case, as Δ_o is incrementally increased, a increases incrementally following the corresponding path in Figure 4. The corresponding values of P may be observed, from Figs. 5 and 6, to decrease accordingly. This process continues, with the strip peeling from its symmetric counterpart in a stable manner, until $a = b_o$. At this point the bending energy of the loop at $s = b^+$ is still sufficiently low as to maintain the bond, while that at $s = b^-$ is large enough to permit debonding. As Δ_o is increased further, the bond point $s = a = b$ then propagates in a stable manner, with the loop shrinking through a series of self-similar shapes until $\ell = \ell_{cr}$, at which point sufficient bending energy exists on both sides of the bond point and the strip separates. For the case where P rather than Δ_o is controlled, the system behaves
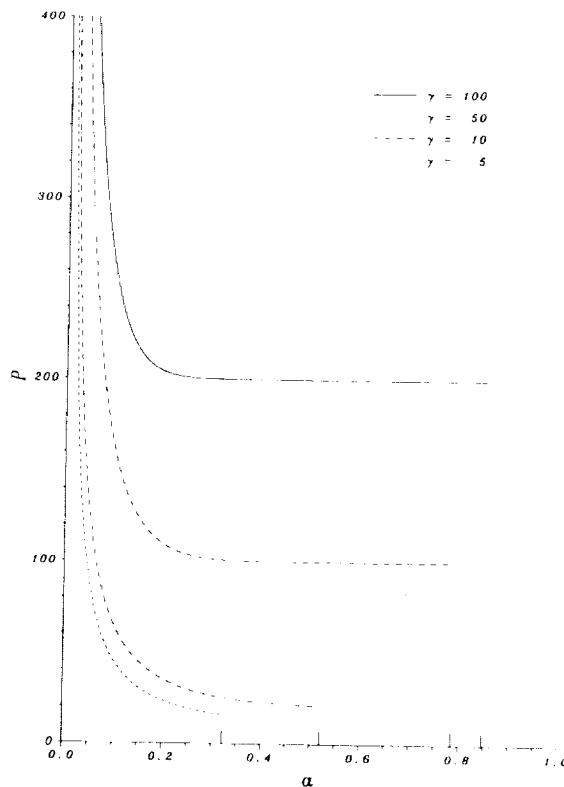

Fig. 5. Lift Zone/Bond Point Propagation Paths ($\gamma = 5$, 10, 50, 100): Applied Load vs. Bond Zone Boundary

80

in an analogous manner except that all behavior during the propagation phases occur in an unstable manner. Thus, for this case the process of complete separation of the elastica is initiated as soon as P reaches a critical value.

The phenomena described above may be observed by simply closing a piece of adhesive tape on itself, thus forming a loop, and then peeling the edges apart. Such an "experiment" would correspond to a deflection controlled test, with the normalized bond energy characterizing the tape observed to be at the upper end of the range of values considered in the numerical simulations presented herein.
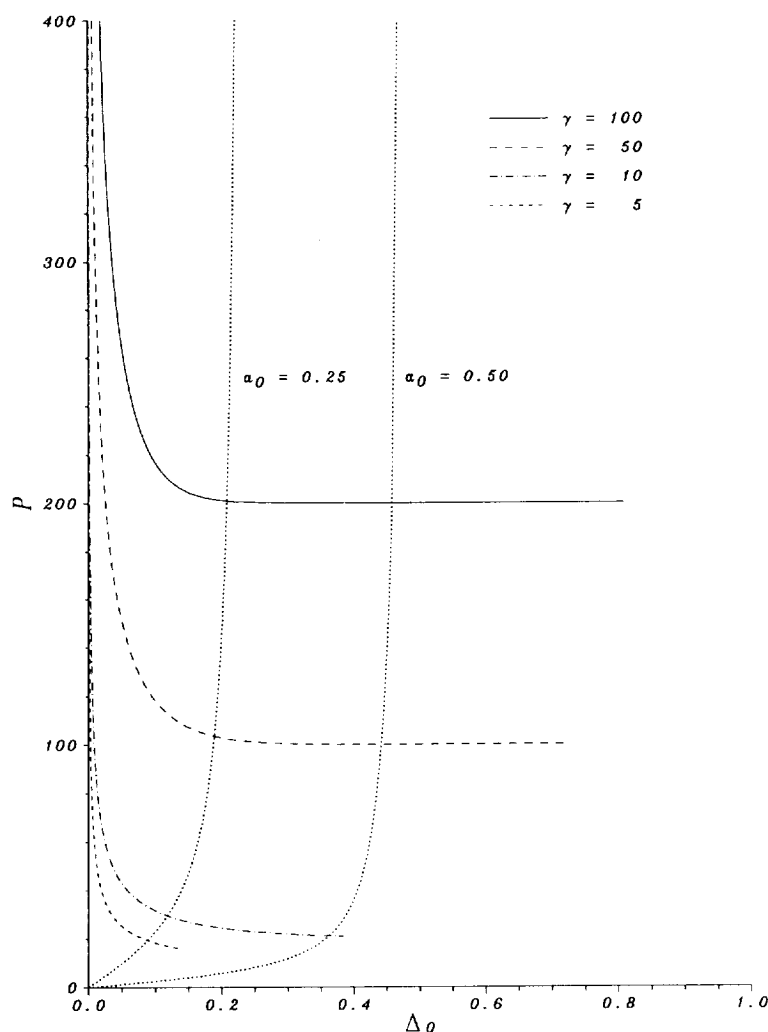
Fig. 6. Prepropagation and Lift Zone/Bond Point Propagation Paths (γ = 5, 10, 50, 100): Applied Load vs. Load Edge Deflection
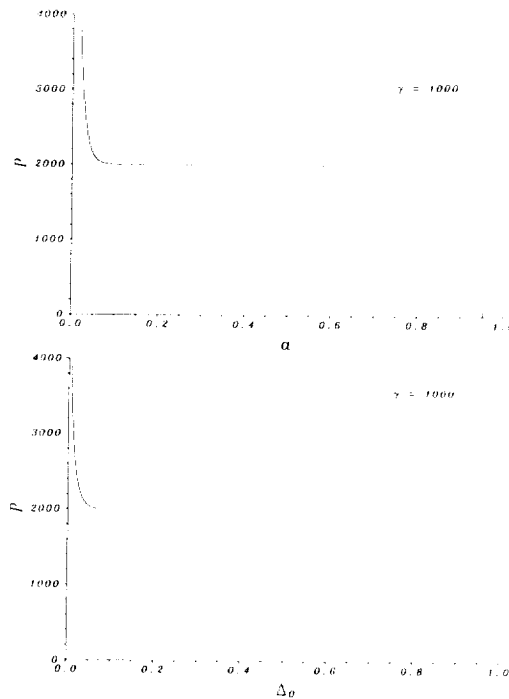
Fig. 7. Lift-Zone/Bond Pt. Propagation Paths ($\gamma = 1000$): (a) Applied Load vs. Bond Zone Boundary, (b) Applied Load vs. Load Edge Deflection
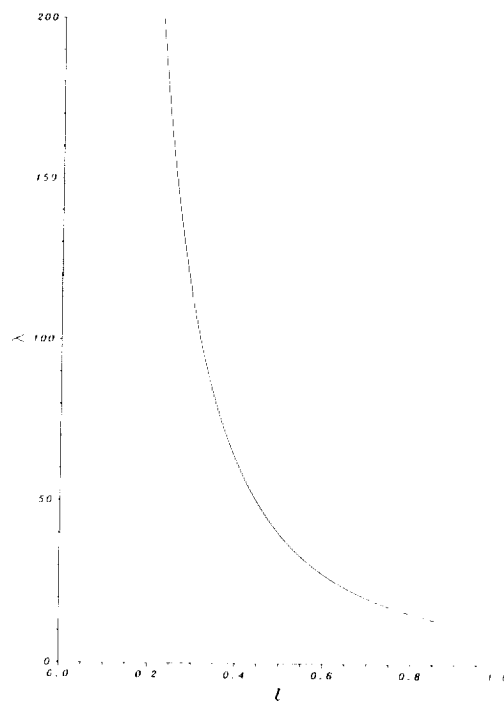

Fig. 8. Internal Force at Inflection Point of Loop as a Function of Loop (Half) Length

References

1. Bottega, W.J.: Peeling of a Cylindrical Layer. Int. J. Fracture, Vol. 38, No. 1, 1988, pp. 3-14.